AD FALCON API Manual

Overview

Javad Ghorbani

March 26, 2026

Contents

1 Overview

This example demonstrates how to initialize a fully coupled solid–water–air analysis for an unsaturated soil domain under gravity loading. The analysis is performed over an 8 m high by 16 m wide domain similar to this example, where body forces are applied to all three phases: solid skeleton, pore water, and pore air.

The objective is to establish a mechanically consistent initial state in terms of stress, pore water pressure, and pore air pressure.

The initialization considers:

- The effect of gravity on each phase through volumetric body forces

- Coupling of pore pressures, void ratio, hysteresis, and saturation using SWRCs

Two modeling approaches are considered:

1. A non-hysteretic SWRC based on the modified van Genuchten model, representing a unique primary drying or wetting path

2. A hysteretic SWRC formulation, incorporating scanning curves to account for historical wetting or drying paths

This setup is useful for simulating realistic initial conditions in unsaturated soils, particularly when analyzing infiltration, evaporation, or loading scenarios where the hydraulic history affects the mechanical response.

1.1 SWRC Assumption (Non-Hysteretic – Modified van Genuchten)

For this baseline, $S_w = S_w(s, e)$ follows a primary drying (or wetting) curve without hysteresis. A common formulation, the Modified van Genuchten model, is given by:

$$S_w = \left(1 + (\alpha_1 \cdot s \cdot e^{\Omega'})^n\right)^{-m} \tag{1}$$

where:
- S_w = degree of saturation
- e = initial void ratio of the soil.
- s = suction.
- α_1, n, Ω' and m are model parameters.
- $S_{w,\min} = 0.0$
- $S_{w,\max} = 1.0$

1.2 Input File Name

fem_coupled_unsat_body_force.txt

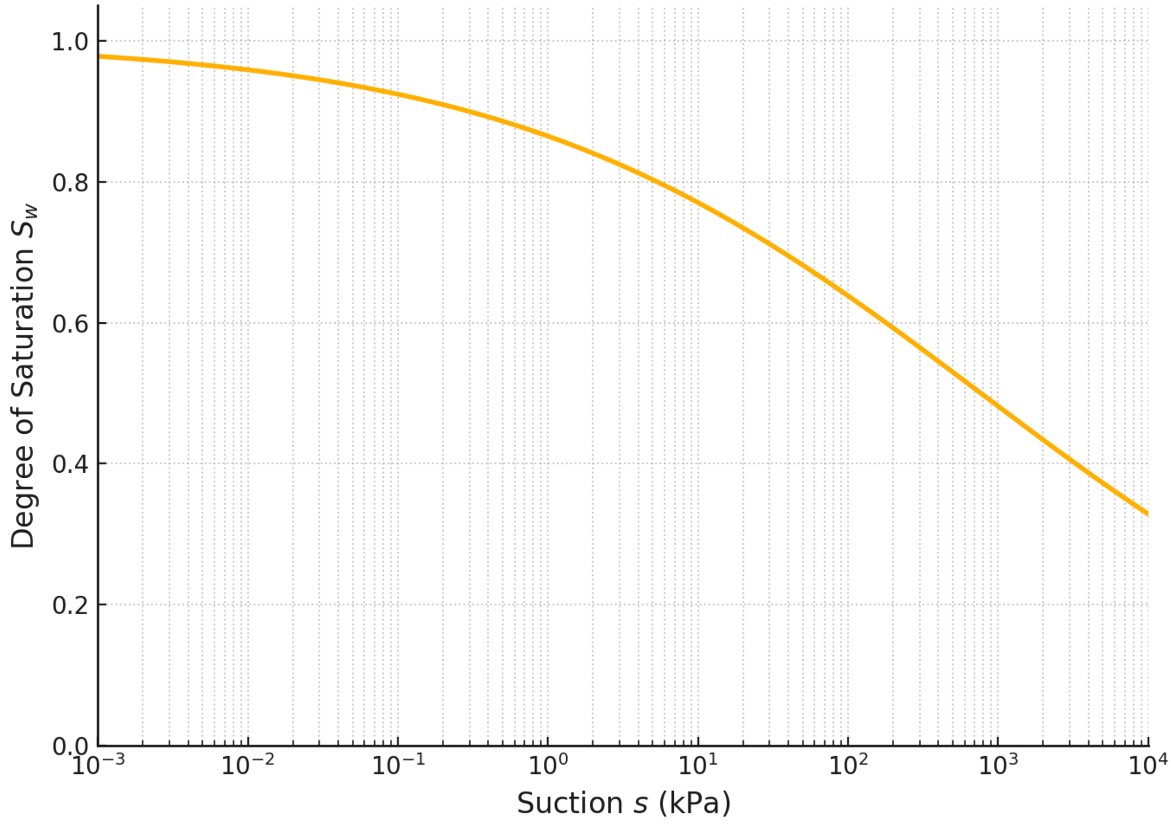

Figure 1: Modified van Genuchten SWRC

Model Parameters

(from `@SWRC: NonHysteretic alpha_1 98 n 0.28 m 0.98 omega_prime 10.6 SW_max 1 SW_min 0`):

- $\alpha_1 = 98$ kPa^{-1}
- $n = 0.28$
- $m = 0.98$
- $e = 0.35 \Rightarrow n_v = 0.259$
- $\omega' = 10.6$ (not used here)

Hysteretic effects and scanning curves are not considered in this example.

1.3 Effective Stress Model

The analysis uses the Ghorbani–Kodikara effective stress formulation, which partitions pore pressure contributions from water and air based on a saturation-dependent weighting:

$$\sigma' = \sigma - S_w^{\left(\frac{\beta_1}{s_w^{\beta_2}}\right)} p_w I - \left(1 - S_w^{\left(\frac{\beta_1}{s_w^{\beta_2}}\right)}\right) p_a I \qquad (2)$$

Model Parameters:

- $\beta_1 = 1.0$
- $\beta_2 = 0.0$

This choice ensures that the model recovers Terzaghi's effective stress in the fully saturated limit $S_w \to 1$.

1.4 Initialization Strategy: Pore Pressure and Effective Stress Fields

To properly initialize the mechanical state of an unsaturated domain under gravity loading, the key is to prescribe consistent initial fields of pore water and pore air pressure. However, typically, the individual values of p_w and p_a are not uniquely important — it is their difference, the matric suction $s = p_a - p_w$, that often governs the hydro-mechanical response of the system.

This typically means multiple combinations of p_w and p_a can produce the same mechanical behavior, provided the resulting suction is the same.

1.5 Example:

- $p_w = -10$ kPa and $p_a = 0$ kPa $\longrightarrow s = 10$ kPa
- $p_w = 90$ kPa and $p_a = 100$ kPa $\longrightarrow s = 10$ kPa
- Both result in identical initial suction field and thus often identical mechanical response in models where suction (not absolute pressures) drives the effective stress and constitutive models.

1.6 Domain Application

In practice, one often prescribes:
- **Uniform air pressure** in the domain (e.g. $p_a = 0$ kPa atmospheric),
- **Matching pore water pressure** (e.g. $p_w = -10$ kPa) to achieve a desired suction (10 kPa),
- This condition is held fixed at the drainage boundary (e.g. surface or top node), while the rest of the domain evolves due to gravity and phase redistribution during the body force

step.

> This ensures drainage equilibrium is enforced at the boundary, while hydrostatic conditions (or gradients from suction profiles) develop naturally in the interior.

1.7 Initial Effective Stress

In addition to prescribing p_w and p_a, FALCOn automatically compute and apply the corresponding initial effective stress field based on the user input.

> **Remark — Near-Surface Adjustment Under Body Force**
> Body force (gravity) acts through element integration (Gauss) points, while effective stress is *only* defined at those points—not directly on the geometric boundary. The first integration point below the surface (its depth depends on element thickness and quadrature) is therefore the first location where the gravity load is assembled. As a result, an *initially prescribed* effective stress field inside the domain may differ slightly near boundary after equilibrium because:
> • The evaluated point is below the boundary (added overburden from the small depth).
> Mesh refinement near the surface reduces this discrepancy by moving the first Gauss point closer to the boundary; a coarse mesh amplifies it. For precise initialization, refine the top layer or use a dedicated gravity-ramp step before applying external actions. ***

We consider three initial pore pressure cases and compute the resulting effective stress using:

Parameters - $\alpha_1 = 98$ kPa^{-1}
- $n = 0.28$
- $m = 0.98$
- $e = 0.35$
- $\Omega' = 10.6$

Pressures - Air pressure fixed: $p_a = 0$ kPa
- Suction: $s = p_a - p_w$, so $p_w = -s$

1.8 Case A: $p_w = 0$ kPa, $p_a = 0$ kPa

- $s = 0$
- $S_w = 1.000000$
- $\chi = 1.000000$

- $\sigma' = 0.00$ kPa

Initial condition: $p_w = 0$ kPa, $p_a = 0$ kPa
Derived quantities: $s = p_a - p_w = 0$, $S_w = 1.0$, $\chi = S_w = 1.0$, $\sigma' = 0.00$ kPa.

Because $S_w = 1.0$ everywhere, the three-phase (solid–water–air) fully coupled formulation collapses to the classical two-phase (solid–water) saturated systemn and the effective stress relation reduces to Terzaghi's form: $\sigma' = \sigma - p_w$ (since $\chi = 1$).

Below we compare the numerical (simulation) profiles with the corresponding analytical (hydrostatic / Terzaghi) lines for **Case A**. Numerical points are shown as filled squares; analytical solutions are dashed lines.

Pore Water Pressure $p_w(z)$	Vertical Effective Stress $\sigma'_v(z)$
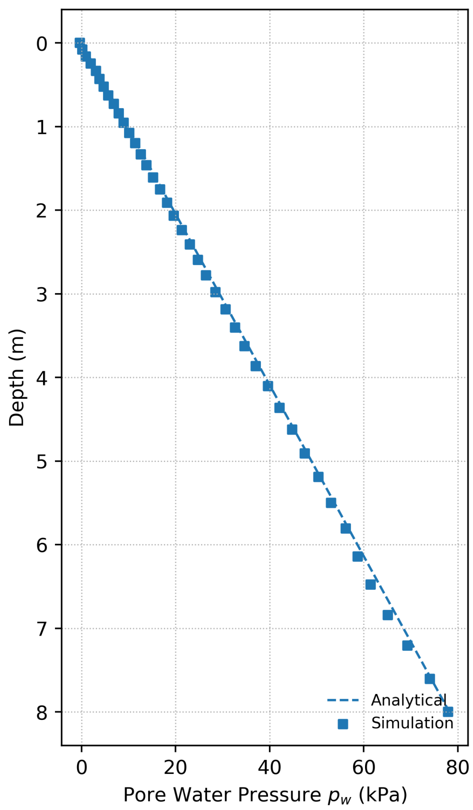	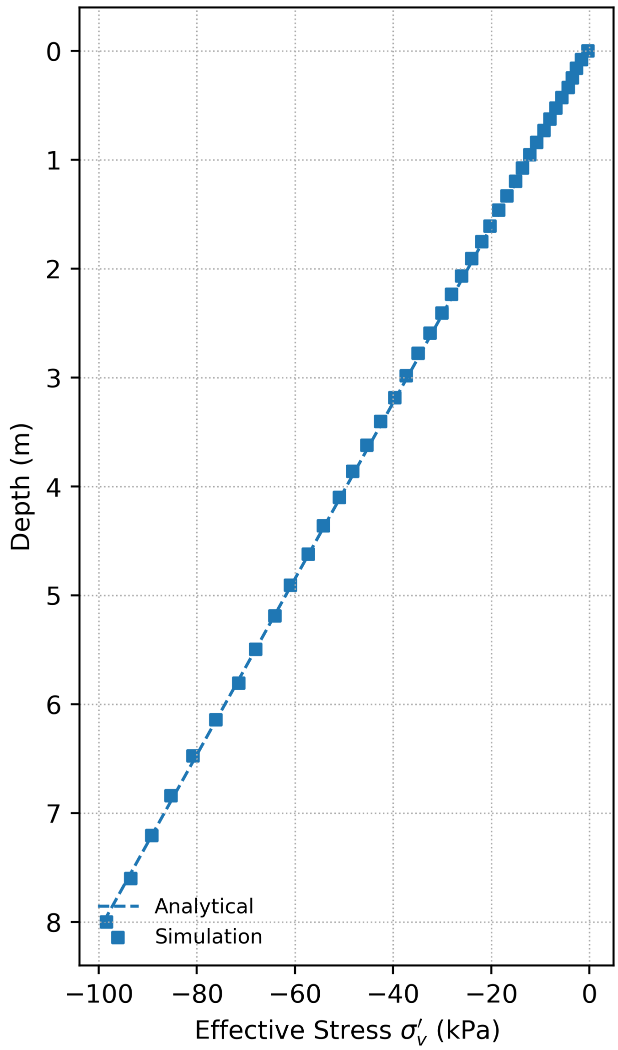

- Water unit weight: $\gamma_w \approx 9.78$ kPa/m

- Saturated unit weight: $\gamma_{\text{sat}} \approx 22.16$ kPa/m
- Effective (submerged) unit weight: $\gamma_{\text{eff}} = \gamma_{\text{sat}} - \gamma_w \approx 12.38$ kPa/m

  These values produce the dashed analytical lines shown.

1.9 Case B: $p_w = -10$ kPa, $p_a = 0$ kPa

- $s = 10$ kPa
- $S_w = (1 + (98 \cdot 10 \cdot 1.82 \times 10^{-5})^{0.28})^{-0.98} = 0.770359$

The figure below (to be inserted) shows the degree of saturation versus depth and pore water pressure versus depth for the initialized unsaturated column. The profile indicates that full saturation is reached at approximately $z \approx 1$ m below the surface (coincident with the transition to non-negative pore water pressure), after which suction-driven desaturation no longer occurs and the pore water pressure follows an approximately linear (hydrostatic) increase with depth.

Saturation Profile	Pore Water Pressure Profile
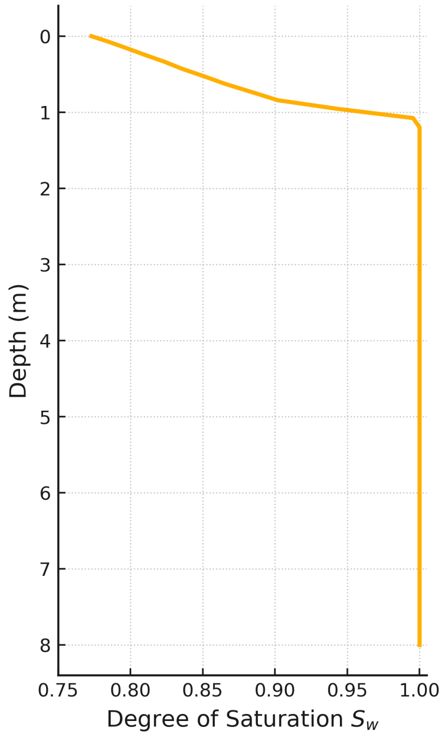	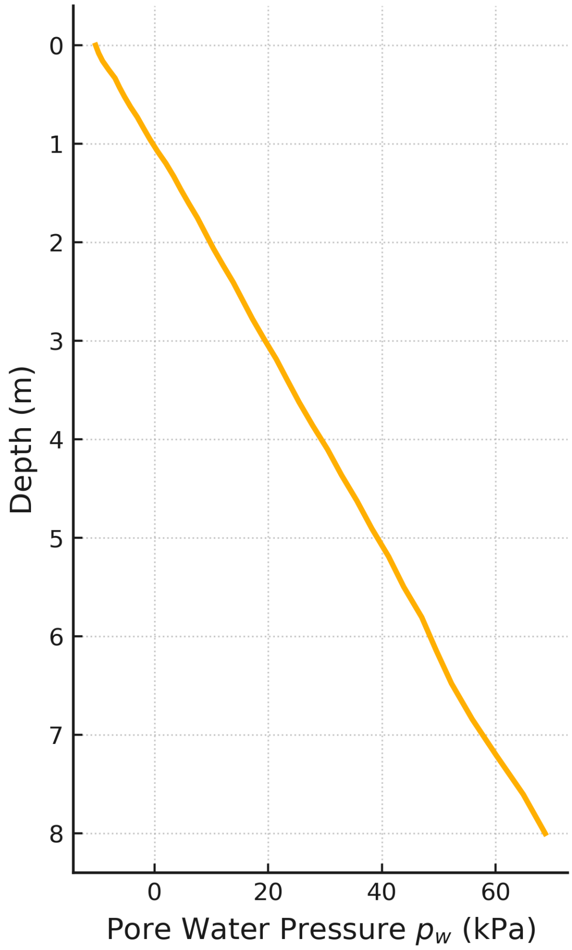

Given:

- Hydrostatic increase below the saturated interface at $z_0 = 1$ m
- Depth of interest: $z = 8$ m
- Water density: $\rho_w = 997$ kg/m^3
- Gravity: $g = 9.81$ m/s^2
- Water unit weight:

$$\gamma_w = \rho_w g = 997 \times 9.81 = 9{,}780.57 \text{ N/m}^3 \approx 9.78 \text{ kN/m}^3 \tag{4}$$

- Gauge pore water pressure at z_0: $p_w(z_0) \approx 0$ kPa (reference at onset of saturation)

Thus pore water pressure at the bottom is roughly obtianed by:

$$p_w(8 \text{ m}) = 9.78 \times 7 = 68.46 \text{ kPa} \tag{5}$$

matching the value obtianed from numerical results.

The below figure shows the total vertical stress σ_v versus depth. A change in slope occurs at approximately $z = 1$ m where $S_w \approx 1$.

Zones: - Upper: $0 \leq z \leq 1$ m - Lower: $z \geq 1$ m

Linear regression form: $\sigma_v(z) = az + b$ applied separately to each zone.

Slopes (compression negative): $a_1 \approx -20.6$ kPa/m (upper), $a_2 \approx -22.1$ kPa/m (lower).

Given $e = 0.35$, porosity $n = \frac{e}{1+e} = 0.2593$, $\rho_s = 2700$ kg/m^3, $\rho_w = 997$ kg/m^3, $g = 9.81$ m/s^2, the saturated unit weight is $\gamma_{\mathrm{sat}} = \left[(1-n)\rho_s + n\rho_w\right]g \approx 22.2$ kN/m^3 which closely matches the magnitude 22.1 kPa/m of the fitted lower slope.

Remark: The difference between slopes is driven by the transition from partially saturated conditions (lower bulk density due to air in pores) above $z \approx 1$ m to fully saturated conditions (higher bulk density) below. Once $S_w \to 1$ the stress gradient approaches the saturated unit weight.

1.10 SWRC with Hydraulic Hysteresis

fem_fcoupled_body_force_hyst

While non-hysteretic models assume a single unique relationship between suction and saturation, real unsaturated soils often exhibit hysteresis: the degree of saturation S_w depends not only on void ratio e and suction s, but also on the wetting or drying history. This is especially critical in cyclic loading, infiltration–evaporation scenarios, or drying–wetting boundary cycles.

To account for this, the hysteretic SWRC introduces an interpolation between the main drying and main wetting curves. To establish the initial hydraulic state which is bounded between the two lines, FALCON uses $\alpha_{p_c} \in [0, 1]$, a state variable that can be initially assigned to the domain by the user.

FALCON uses the hysteretic modified van Genuchten equation to represent this hysteresis as:

$$S_w = \left(1 + (\alpha_2 \cdot s \cdot e^{\Omega'})^n\right)^{-m} + \alpha_{p_c}\left[\left(1 + (\alpha_1 \cdot s \cdot e^{\Omega'})^n\right)^{-m} - \left(1 + (\alpha_2 \cdot s \cdot e^{\Omega'})^n\right)^{-m}\right] \tag{3}$$

Where:

- α_1 = drying curve fitting parameter
- α_2 = wetting curve fitting parameter

Main wetting and **main drying** curves:

- $\alpha_{p_c} = 0 \to$ main wetting
- $\alpha_{p_c} = 1 \to$ main drying
- $0 < \alpha_{p_c} < 1 \to$ scanning path (intermediate state)

The figure below shows the main drying and wetting curves and the influence of α_{p_c} at a suction value of 100 kPa and a void ratio of 0.35, assuming α_1 is half of α_2 (i.e., $\alpha_1 = 98$ and

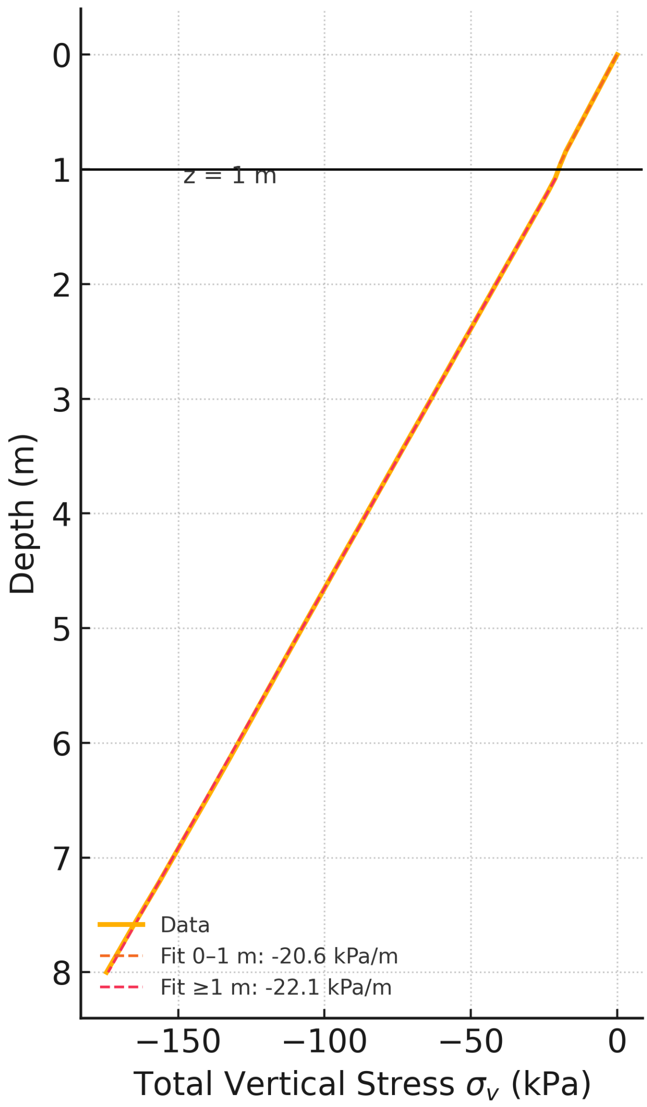

Figure 2: Total Vertical Stress vs Depth

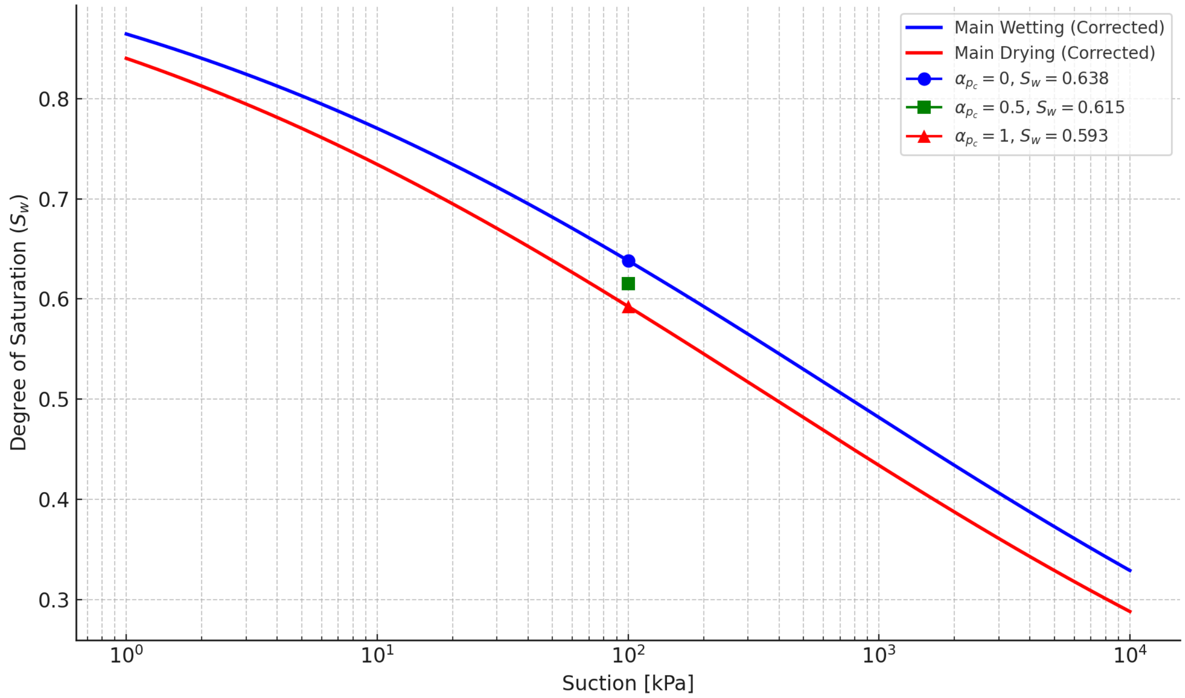

Figure 3: Hysteresis SWRC

$\alpha_2 = 196$) kPa^{-1}. All other parameters—$n = 0.28$, $m = 0.98$, and $\Omega' = 10.6$—are the same as in the previous examples.

To examine the effect of α_{p_c} on the hydrostatic state, we compare three cases, each using a constant initial value of the hysteresis parameter α_{p_c}:

- $\alpha_{p_c} = 0 \rightarrow$ pure main wetting
- $\alpha_{p_c} = 1 \rightarrow$ pure main drying
- $\alpha_{p_c} = 0.5 \rightarrow$ midpoint (scanning state)

The domain is initialized with a uniform pore water pressure of -100 kPa, zero pore air pressure, and void ratio $e = 0.35$. These variations directly impact the initial effective stress and hydro-mechanical response during gravity initialization and subsequent loading.

Degree of Saturation vs Depth

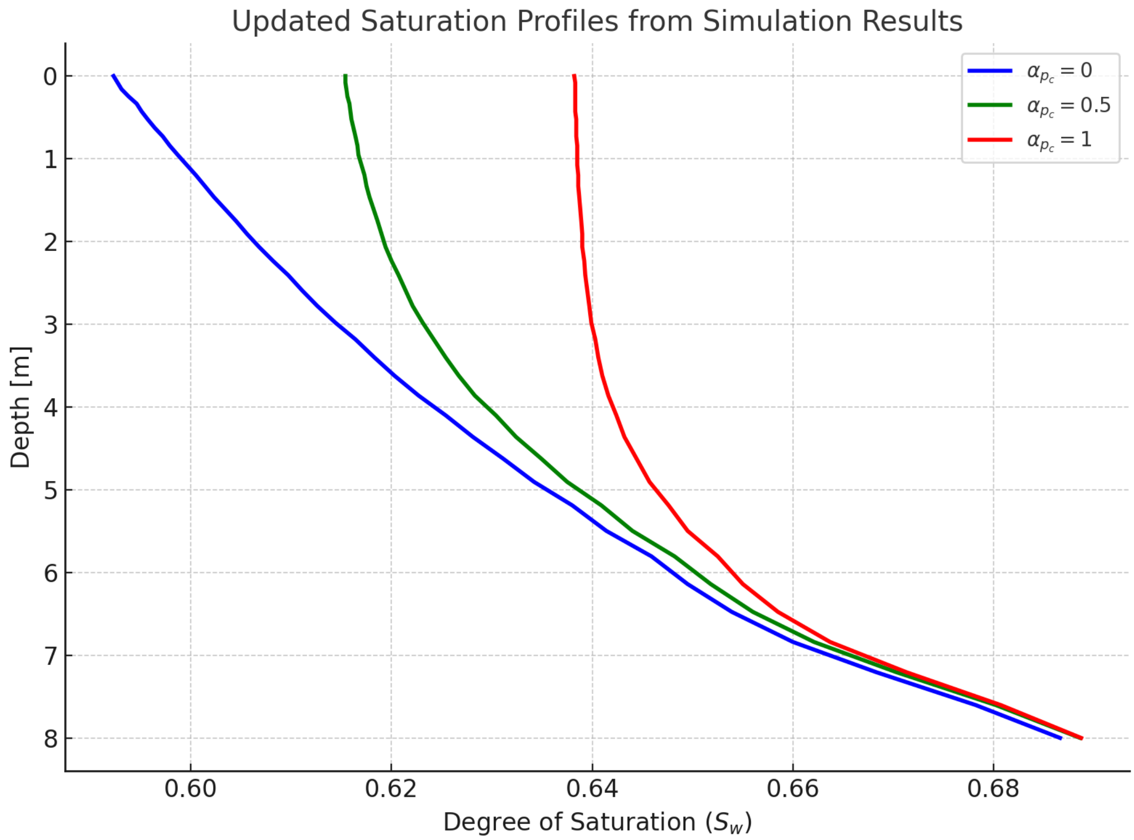

Remark:
When using hydraulic hysteresis, the solution typically exhibits strong nonlinearity. This is because the SWRC is no longer analytical and often involves internal numerical integration or lookup schemes to interpolate between wetting and drying branches.
Therefore: - Extra care must be taken when choosing time step size and solver tolerances.
- The hydrostatic equilibrium state should be manually verified, particularly when initializing the system under gravity loading.
- It is also recommended to monitor the convergence behavior during early simulation steps and refine mesh or time control settings as needed.